An experimental approach for determining unsaturated hydraulic properties of rock fractures

Hu Yunjin[1]*, Su Baoyu[2] and Mao Genhai[1]

[1]Zhejiang University, College of Civil Engineering and Architecture, Hangzhou 310027, China
Tel: +86 571 8795 1356; fax: + 86 571 8795 1356; *Corresponding author
E-mail: *huyunjin@tsinghua.org.cn*
[2]Hohai University, College of Water Conservancy and Hydropower Engineering, Nanjing, China

Received 29 August 2002; accepted in revised form 9 January 2004

Abstract An experimental approach for determining the unsaturated hydraulic properties (the relations between capillary pressure, saturation and unsaturated hydraulic conductivity) of rock fractures is developed and tested. Applying this approach to a single fracture, and with only water flowing, the capillary pressure–saturation and unsaturated hydraulic conductivity–capillary pressure relationships of the fracture during drainage and imbibition can be determined simultaneously. To facilitate the test of the validity of the experimental approach and to elucidate the characteristics of water flow in unsaturated fractures, an analogous fracture with parallel, connected channels of different apertures was fabricated. Experiments of unsaturated water flow in the analogous fracture were carried out. Some characteristics of water flow in unsaturated fractures (hysteresis between drainage and imbibition, etc.) were elucidated. Comparison of measured saturation values and theoretical saturation values corresponding to different apertures at the beginning of drainage and imbibition shows that the experimental approach presented in this paper is valid.

Keywords Analogous fracture; experimental approach; rock fracture; unsaturated hydraulic properties

Nordic Hydrology **Vol 35 No 3 pp 251–260** © IWA Publishing 2004

Introduction

Modeling water flow in unsaturated fractured rocks is of interest in many areas of active research (Liu and Bodvasson 2001). Water flow in fractured rocks is often dominated by the highly permeable pathways provided by fractures (Bear *et al.* 1993). The numerical methods for modeling water flow in variably saturated porous media have often been borrowed to simulate water flow in unsaturated fractured rocks since water flow in unsaturated fractured rocks is usually described by Richards' equation (Peters and Klavetter 1988; Hu *et al.* 2001). Therefore, the determination of relations between capillary pressure, saturation and unsaturated hydraulic conductivity of a single fracture is most important when modeling water flow in unsaturated fractured rocks. Many experiments have been carried out to obtain reliable unsaturated hydraulic properties of fractures.

Romm (1966) studied the two-phase flow of water and kerosene in artificial parallel-plate fractures. He measured linear relative permeabilities, but this is not necessarily representative of the two-phase relative permeabilities in real fractures with a variable aperture distribution. Merrill (1975) conducted steady state relative permeability experiments similar to Romm's on glass plates and sandstone blocks. He found that wetting phase saturations clustered around a value of $\sim$0.72 and 0.62 for the glass plates and sandstone fracture, respectively, for almost the whole range of flow rates studied. Fourar *et al.* (1993) studied the two-phase flow of water and air in parallel glass plates, both smooth and roughened by gluing on glass beads. The results were strong nonlinear functions of saturation and flow rate when analyzed as a relative permeability. Pieters and Graves (1994) performed displacement experiments to obtain the relative permeability ratio and determined saturations from videotaped images. The images showed channeling and a large amount of

fingering prior to breakthrough. Nicholl and Glass (1994) measured the wetting phase relative permeability on analogous fractures made from two sheets of textured plate glass and found that relative permeability was proportional to saturation to the third power. Reitsma and Kueper (1994) developed a laboratory technique to measure capillary pressure and saturation for a single fracture under different states of normal stress. The method was applied to an induced, rough-walled rock fracture in limestone using water and oil as the wetting and nonwetting phases, respectively. Capillary pressure was plotted against the volume of wetting phase imbibed or displaced by the nonwetting phase. Persoff and Pruess (1995) measured the relative permeability for natural rock fractures and transparent replicas of natural fractures using gas and water. Relative permeability was plotted against the mass flow rate ratio. Relative permeabilities in this experiment did not fit a linear or Corey-type (power law) model. Bertels *et al.* (2001) developed an experimental technique using computed tomography scanning to measure aperture distribution and *in situ* saturation along with capillary pressure and relative permeability for the same rough-walled fracture. This technique was applied to an induced fracture in a cylindrical basalt core. They found that the water relative permeability showed a sharp change over a narrow range of average water saturation. Indraratna and Ranjith (2001) designed a new apparatus for examining the strength and permeability characteristics of fractured and intact rocks under two-phase flows. Tests were conducted on fractured granite rocks subjected to axial and confining pressure, and the results showed that Darcy's law could be modified for estimating two-phase flow rates using the relative permeability concept.

Two phases flowed simultaneously in fractures in the experiments reviewed above except in the experiment of Nicholl and Glass, but they only measured relative permeability to liquid at varying degrees of desaturation. However, the use of Richards' equation to describe unsaturated water flow implies that the gas phase acts as a passive bystander during water flow (Pruess 1998). Therefore, it is inappropriate to use relations between capillary pressure, saturation and relative permeability determined by the aforesaid two-phase flow and displacement experiments as the unsaturated hydraulic properties of fractures. For this reason, an experimental approach for determining the unsaturated hydraulic properties of fractures was developed in this paper.

The main purposes of the present work are: 1) introduction of the experimental approach for determining unsaturated hydraulic properties of fractures, 2) a test of the validity of the experimental approach, and 3) elucidation of the characteristics of water flow in unsaturated fractures. For convenience, an analogous fracture with parallel, connected channels of different apertures was fabricated and experiments of unsaturated water flow in the fracture were conducted. In all experiments, the gas phase acted as a bystander during water flow.

Experimental approach

Analogous fracture characterization

As is illustrated in Figure 1, the analogous fracture consisted of two steel plates clamped together. The lower plate was smooth, whereas five steps with different depths were excavated on the upper plate. Thus, the analogous fracture has five parallel, connected channels of different apertures and can approximately simulate natural fractures. The left and right sides of the analogous fracture were sealed using epoxy (see Figure 1).

It would be more interesting if the changes in pore dimension were made in the longitudinal direction since it is more likely to represent natural fractures than the analogous fracture adopted here. Because one of the main purposes of the present work is to test the validity of the experimental approach, a simple analogous fracture is adopted to facilitate the test. However, complicated analogous fractures can be fabricated and experiments on them can be conducted by the same means as presented here.

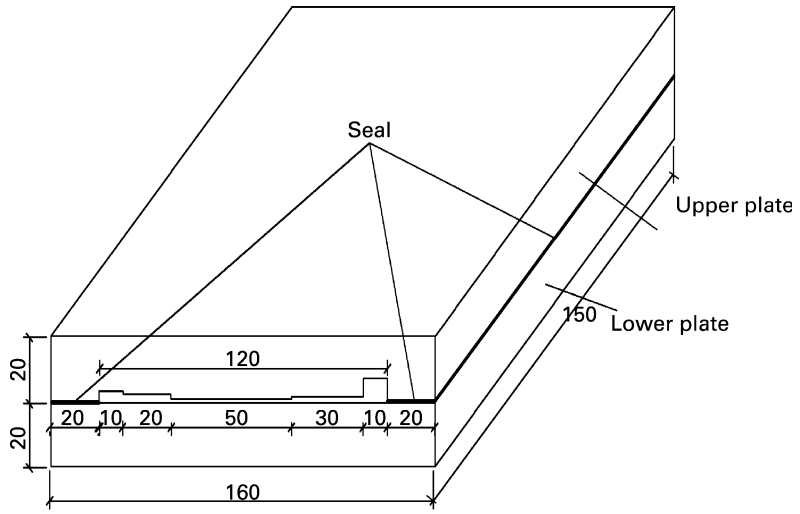

Figure 1 Schematic drawing of the analogous fracture (all units are given in mm)

From left to right, the five different aperture values of the analogous fracture are 0.104 mm, 0.076 mm, 0.024 mm, 0.047 mm and 0.198 mm. The length, width and weighted average aperture of the analogous fracture are 150.0 mm, 120.0 mm and 0.0596 mm, respectively. The weighted average aperture is determined by dividing the sum of the fracture volume by the sum of the fracture area. The total volume of water in the analogous fracture is 1.073 cm^3 when it is saturated. From left to right, the saturated water volumes corresponding to the five channels of different apertures are 0.156 cm^3, 0.228 cm^3, 0.180 cm^3, 0.212 cm^3 and 0.297 cm^3.

Experimental apparatus

A schematic diagram of the experimental apparatus is shown in Figure 2. The experimental apparatus is made of the following four parts: 1) a constant-head water supply system including a Mariotte bottle and high-precision electronic balance *a*; 2) a test cell including the analogous fracture, capillary barriers, end caps and tensiometers; 3) an elevator system used to move the analogous fracture up and down; and 4) a constant-head water collecting system including plexiglass tubes and high-precision electronic balance *b*.

The end caps were sealed to the analogous fracture ends using O-rings. They were fabricated to ensure that the gas phase in the analogous fracture is open to atmospheric pressure and to measure the inlet and outlet pressures of water. The capillary barriers were used to minimize capillary end effects. The capillary barrier was composed of a mixture of water, cement and sand in a ratio of 1.33:1:5 by weight. The sand was sieved to fall between a 35 and 60 mesh. The air entry pressure of the capillary barrier was measured to be 180 cm of water, which was sufficient for the expected range of capillary pressures. A detailed schematic drawing of the end caps and the capillary barriers is shown in Figure 3. The gas phase in the analogous fracture was open to atmospheric pressure through vertical grooves in the capillary barriers and two holes in the end caps (see Figure 3). These capillary barriers and grooves are similar to those used by Persoff and Pruess (1995). Therefore, the gas phase in the analogous fracture was at atmospheric pressure with only water flowing in all experiments. In order to bypass the pressure drop across the capillary barrier, pressure was measured through a separate mortar-filled tensiometer directly in contact with the analogous fracture. The tensiometer has a range of operation from -100 cm of water to $+100$ cm of water. Its resolution is 0.1 cm of water. The Mariotte bottle was used to supply water to the

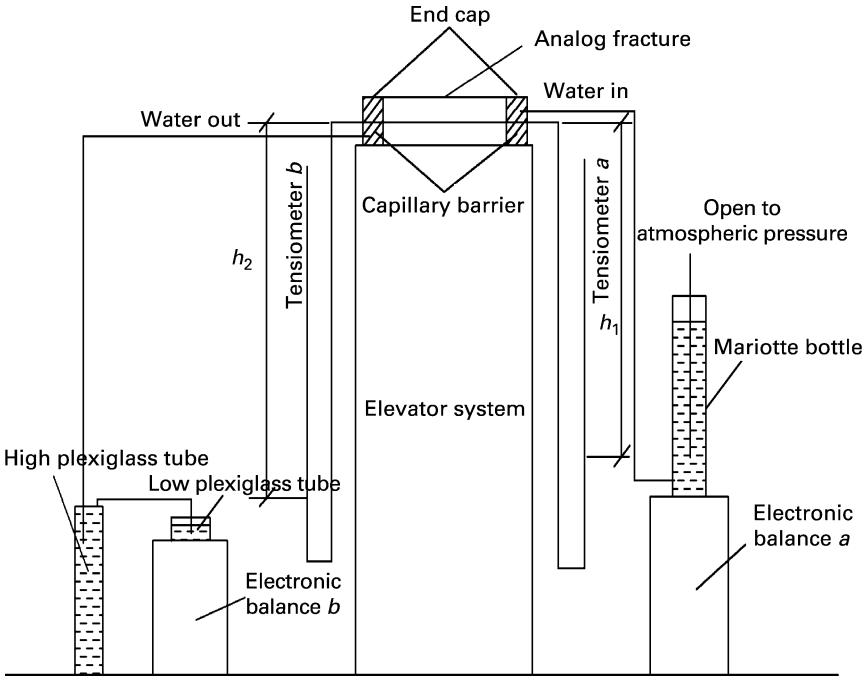

Figure 2 Schematic diagram of the experimental apparatus for unsaturated water flow in the analogous fracture (A detailed drawing of the analogous fracture, end caps and capillary barriers is presented in Figure 3)

analogous fracture while keeping a constant water head. The water collecting head was kept constant by fixing the elevation of the high plexiglass tube. The electronic balance *a* was used to measure the weight of supplied water, while the electronic balance *b* was used to measure the weight of collected water. The electronic balances were made by Shanghai balance manufacturer. They both have a range of operation from 0–350 g. Their resolutions are both 0.01 g. Gravitational effects were minimized by orienting the analogous fracture horizontally.

Experimental principles

The capillary pressure–saturation and unsaturated hydraulic conductivity–capillary pressure relationships of the analogous fracture were determined on the principle of kinetic equilibrium, i.e. on the establishment of successive states of the steady flow of water by

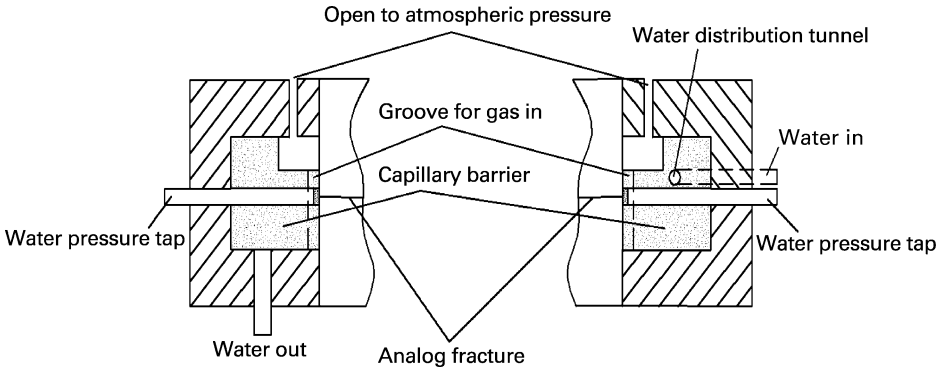

Figure 3 Detailed schematic drawing of end caps and capillary barriers

changing the capillary pressure in the analogous fracture. The capillary pressure was changed by adjusting the elevation of the analogous fracture. The basic principles are as follows.

The capillary pressure corresponding to a certain elevation of the analogous fracture is

$$h_c = \frac{h_1 + h_2}{2} \tag{1}$$

where h_1 and h_2 are the capillary pressures at the inlet and the outlet of the analogous fracture, respectively, and h_c represents the average capillary pressure for the analogous fracture. The differential water pressure at either end of the fracture is required to maintain flow through the fracture; however, this leads to a variable distribution of capillary pressure throughout the fracture. Since the difference between h_1 and h_2 is small, the difference in aperture is greater than the change in capillary pressure induced across the fracture. Therefore, the impact of the errors introduced by using a variable capillary pressure in the fracture and assigning the average capillary pressure to represent the pressure condition is negligible.

When the analogous fracture is lifted (or lowered) from elevation 1 (corresponding to capillary pressure h_{c1}) to elevation 2 (corresponding to capillary pressure h_{c2}), according to capillary theory, water will be removed from (or drawn into) the analogous fracture. Let gw_1, gw_2,..., gw_n represent the water supply volumes during n adjacent time intervals from the beginning of the lift (or lowering) to the flow in the analogous fracture reaching a new steady state. The water supply volume during a given time interval is calculated according to the difference in the reading of electronic balance a between the initial time interval and the end time interval. Let jw_1, jw_2,..., jw_n represent the water collecting volumes during n adjacent time intervals from the beginning of the lift (or lowering) to the flow in the analogous fracture reaching a new steady state. The water collecting volume during a given time interval is calculated according to the difference in the reading of electronic balance b between the initial time interval and the end time interval. Let zw_1, zw_2,..., zw_n represent the changes in the volume of water in the tensiometers during n adjacent time intervals from the beginning of the lift (or lowering) to the flow in the analogous fracture reaching a new steady state. The change in the volume of water in the tensiometers during a given time interval is calculated according to the change in water levels in the tensiometers between the initial time interval and the end time interval. According to the principle of water balance, the drain discharge (or soakage) corresponding to capillary pressure h_{c2} is

$$\Delta\theta = |(jw + zw) - gw| \tag{2}$$

where $jw = jw_1 + jw_2 + \ldots + jw_n$, $zw = zw_1 + zw_2 + \ldots + zw_n$, $gw = gw_1 + gw_2 + \ldots + gw_n$.

According to the total volume of water in the analogous fracture and the aforesaid drain discharge (or soakage), the saturation corresponding to capillary pressure h_{c2} can be calculated. Therefore, the relationship between capillary pressure and saturation can be obtained by changing the elevation of the analogous fracture (thus changing the capillary pressure).

For each capillary pressure, the water volume passing through the analogous fracture during a given time interval can be measured after a steady state of water flow is reached. According to Darcy's law, the hydraulic conductivity of the analogous fracture at each capillary pressure can be calculated. The formula used to calculate hydraulic conductivity is

$$k = \frac{wl}{tab(h_2 - h_1)} \tag{3}$$

where w is the water volume passing through the analogous fracture during the time interval t (cm^3), l is the length of the analogous fracture (cm), a is the width of the analogous

fracture (cm), b is the weighted average aperture of the analogous fracture (cm) and h_1 and h_2 are the same as those of Eq. (1).

Experimental procedures

Experiments on unsaturated water flow in the analogous fracture were carried out under constant temperature (20°C). The experimental procedures are as follows.

(1) The apparatus was evacuated to a pressure above the vapor pressure of water, and deaired water was injected to saturate the capillary barriers and the analogous fracture.
(2) The water supply head and the water collecting head were fixed, which was achieved by fixing the elevations of the Mariotte bottle and the high plexiglass tube. Using the elevator system, the analogous fracture was lowered such that the water pressure in the fracture was positive. The water volume passing through the analogous fracture during a given time interval was measured and water levels in the tensiometers were recorded. The saturated hydraulic conductivity of the analogous fracture was calculated according to Eq. (3).
(3) Capillary pressure values, here called forecast values of capillary pressure, corresponding to different apertures at the beginning of drainage or imbibition were calculated according to Laplace's equation, based on the contact angle of the steel–water–gas interface, the interfacial tension of the water–gas interface and the five different aperture values of the analogous fracture.
(4) Consulting the forecast value of the air entry capillary pressure corresponding to the largest aperture, the analogous fracture was lifted such that the capillary pressure in the fracture was 2.0 cm of water less than the forecast value. Water supply volumes, water collecting volumes and water levels in the tensiometers were subsequently recorded every half hour. Meanwhile, the difference between the water supply volume and the sum of the water collecting volume and the change in the volume of water in the tensiometers was calculated. Three adjacent differences were added up. If it was less than 0.01 cm^3, drainage was considered not to have begun. The analogous fracture was lifted in small increments of 0.1 cm of water (the turbine of the elevator system circumrotates once; the fracture is just lifted (or lowered) by 0.1 cm) until the sum of the three adjacent differences was equal to or greater than 0.01 cm^3.
(5) Recording of water supply volumes, water collecting volumes and water levels in the tensiometers continued every half hour until a steady state of water flow was reached (once the water supply volume was equal to the water collecting volume during the same time interval, it would be considered that a steady state of water flow had been reached). Then, h_1 and h_2 were recorded and h_c was calculated according to Eq. (1). The drain discharge corresponding to this capillary pressure was obtained according to Eq. (2). According to the total volume of water in the analogous fracture, the saturation corresponding to this capillary pressure was calculated.
(6) The water volume passing through the analogous fracture was measured after a steady state of water flow was reached. The unsaturated hydraulic conductivity corresponding to this capillary pressure was calculated according to Eq. (3).
(7) The analogous fracture was lifted, consulting the forecast values of capillary pressure step by step. Steps (4)–(6) were repeated and the capillary pressure–saturation and unsaturated hydraulic conductivity–capillary pressure relationships during drainage were obtained.
(8) Following the above-mentioned principles, the analogous fracture was lowered stepwise to obtain the capillary pressure–saturation and unsaturated hydraulic conductivity–capillary pressure relationships during imbibition.

Experimental results and discussion

Saturation values corresponding to different apertures of the analogous fracture at the beginning of drainage and imbibition were calculated theoretically to test the validity of the aforesaid experimental approach. According to capillary theory, water will be removed from progressively smaller aperture regions of the analogous fracture at higher capillary pressure during drainage and drawn into progressively larger aperture regions of the analogous fracture at lower capillary pressure during imbibition. The drain discharge or soakage of different apertures is equal to the saturated water volume corresponding to different apertures. Thus, according to the total volume of water in the fracture and the cumulative drain discharge or soakage, theoretical saturation values corresponding to different apertures at the beginning of drainage and imbibition can be calculated. The detailed description of the method for calculating theoretical saturation values is also described by Hu (2001). Theoretical saturation values of the five different apertures at the beginning of drainage and imbibition are shown in Table 1. For convenience of comparison, the corresponding measured saturation values are also listed in Table 1.

Table 1 shows that measured saturation values are close to the theoretical values. During drainage, the difference between the measured saturation value and theoretical saturation value is caused by the following two reasons: 1) theoretical saturation values disregard the effects of hygroscopic water and film water, and 2) measured aperture values of the analogous fracture are not exactly equal to the real aperture values because of measurement error. One additional source of error during imbibition is that the theoretical saturation values disregard the effects of bound water after drainage and trapped gas during imbibition.

These results demonstrate that the experimental approach presented herein is valid.

Based on the experimental data, the capillary pressure–saturation and unsaturated hydraulic conductivity–capillary pressure relation curves of the analogous fracture during drainage and imbibition are presented in Figures 4 and 5. The capillary pressure–saturation and unsaturated hydraulic conductivity–capillary pressure relation curves are step functions in reality because aperture size does not change continuously but rather stepwise. For convenience, however, the aforesaid curves are smoothed.

Figure 4 shows that there is entry pressure during drainage. Since the largest aperture of natural fractures is usually larger than that of the analogous fracture, the entry pressure of natural fractures will be smaller than that of the analogous fracture. When the capillary pressure reaches 51.1 cm of water, the analogous fracture still has a certain water saturation that is here called the irreducible saturation. Here, water corresponding to the irreducible saturation is hygroscopic water and film water because the smallest aperture region of the analogous fracture is drained when the capillary pressure reaches 38.44 cm of water. In natural fractures, water corresponding to the irreducible saturation includes water in very small aperture regions and trapped water, besides hygroscopic water and film water. Therefore, the irreducible saturation of natural fractures may be larger than that of the

Table 1 Measured and theoretical saturation values of different apertures beginning drainage and imbibition

		Saturation				
Drainage	Measured value	1.0	0.729	0.589	0.384	0.189
	Theoretical value	1.0	0.723	0.578	0.365	0.168
	Relative difference	0.0%	0.82%	− 1.87%	4.95%	11.11%
Imbibition	Measured value	0.990	0.711	0.571	0.366	0.180
	Theoretical value	1.0	0.723	0.578	0.365	0.168
	Relative difference	− 1.01%	− 1.69%	− 1.23%	0.27%	6.67%

Note: relative difference $= \frac{\text{measured value} - \text{theoretical value}}{\text{measured value}} \times 100\%$.

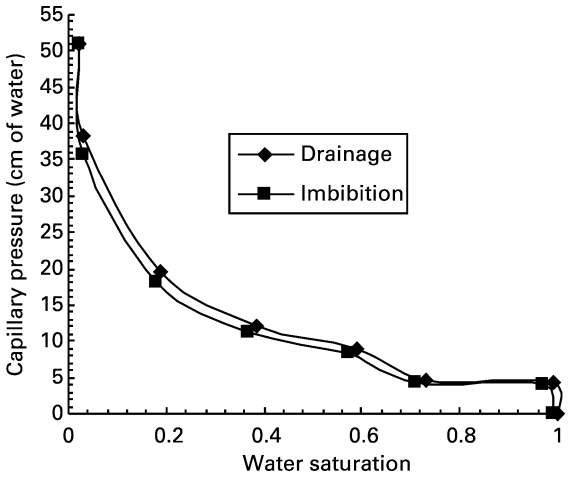

Figure 4 Capillary pressure–saturation relation curves during drainage and imbibition

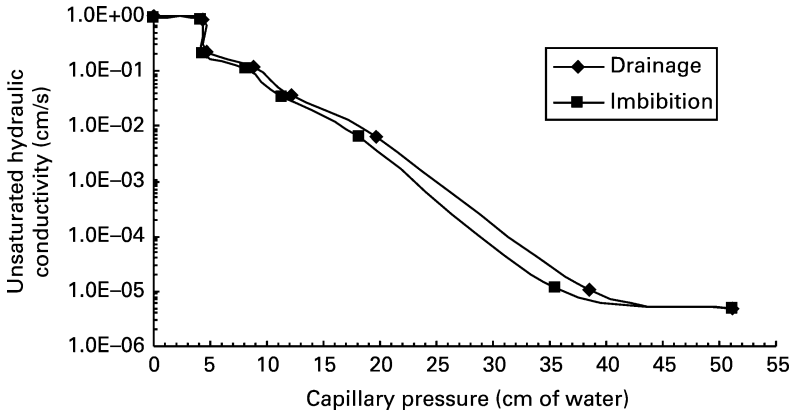

Figure 5 Unsaturated hydraulic conductivity–capillary pressure relation curves during drainage and imbibition

analogous fracture. During imbibition, there is residual gas saturation in the analogous fracture. This is because the lower and upper plates are not absolutely smooth and there are large aperture regions surrounded by small aperture regions. Thus, gas entrapment is inevitable during imbibition. Because the aperture of natural fractures changes continuously and the aperture distribution of natural fractures is more complicated than that of the analogous fracture, residual saturation of natural fractures will be larger than that of the analogous fracture.

Figure 5 shows that the unsaturated hydraulic conductivity of the analogous fracture is not zero even if the smallest aperture region is drained or is not imbibed. This is because film water participates in flow. Thus the contribution of film water to unsaturated hydraulic conductivity cannot be ignored, which confirms the experimental results of Tokunaga and Wan (1997).

Figures 4 and 5 illustrate that there is hysteresis between drainage and imbibition. That is, for the same capillary pressure, the saturation and unsaturated hydraulic conductivity of drainage are larger than those of imbibition. Hysteresis is often caused by the raindrop effect (hysteresis in the contact angle) and the ink-bottle effect (Dullien 1992). Because the upper and lower plates of the analogous fracture are very smooth, the analogous fracture made

by overlapping them does not have any bottleneck pore space. Therefore, hysteresis caused by the ink-bottle effect can be neglected and hysteresis of the analogous fracture is mainly caused by hysteresis in the contact angle. Therefore, hysteresis in the water retention curve of natural fractures is likely to be greater than that of the analogous fracture. The larger the saturation, the larger the flow area. Therefore, for the same capillary pressure, the unsaturated hydraulic conductivity of drainage is larger than that of imbibition. Because hysteresis in the water retention curve of natural fractures may be greater than that of the analogous fracture, hysteresis in the unsaturated hydraulic conductivity–capillary pressure relation curve of natural fractures may be greater than that of the analogous fracture.

Conclusions

The experimental approach for determining the unsaturated hydraulic properties of fractures presented herein is valid. The capillary pressure–saturation and unsaturated hydraulic conductivity–capillary pressure relationships during drainage and imbibition can be determined simultaneously using this experimental approach. Through the analysis of experimental results on unsaturated water flow in the analogous fracture, the following conclusions can be drawn.

(1) There is entry pressure and irreducible saturation during drainage and there is residual gas saturation during imbibition.
(2) There is hysteresis in the capillary pressure–saturation and unsaturated hydraulic conductivity–capillary pressure curves caused by hysteresis in the contact angle.
(3) The effects of hygroscopic water and film water on the water retention curve are noticeable. The contribution of film water to the unsaturated hydraulic conductivity cannot be neglected, especially when water saturation is very small. Numerical simulation methods for determining unsaturated hydraulic properties of fractures in the literature all disregard the effects of hygroscopic water and film water (Kwicklis and Healy 1993), so the simulation models need to be revised according to these experimental results.
(4) Capillary theory, which is the foundation of numerical simulation methods, is valid. But the effects of water entrapment and gas entrapment should be considered when generating water-filled areas of fracture. The contributions of hygroscopic water and film water to saturation and film water to unsaturated hydraulic conductivity should be considered.

In this paper, the experimental approach introduced to determine the unsaturated hydraulic properties has only been applied to an analogous fracture. Experiments on unsaturated water flow in natural fractures have not been done. Models for the capillary pressure–saturation and unsaturated hydraulic conductivity–capillary pressure relationships of fractures have not been fitted due to the lack of measured data. At present, models developed for porous media have often been borrowed to represent the unsaturated hydraulic properties of fractures while their usefulness and limitations have not been investigated. Using the experimental approach presented herein and replacing the analogous fracture by natural fractures, experiments on unsaturated water flow in natural fractures can be conducted and models representing the unsaturated hydraulic properties of fractures can be tested based on the experimental results.

Acknowledgement

This research was supported financially by the Key Program of National Natural Science Foundation of China (grant no. 50239070).

References

Bear, J., Tsang, C. and de Marsily, G. (1993). *Flow and Contaminant Transport in Fractured Rock*, Academic, New York, 559–560.

Bertels, S.P., DiCarlo, D.A. and Blunt, M.J. (2001). Measurement of aperture distribution, capillary pressure, relative permeability, and in situ saturation in a rock fracture using computed tomography scanning. *Water Resources Res.*, **37**(3), 649–662.

Dullien, F.A.L. (1992). *Porous Media: Fluid Transport and Pore Structure*, Academic, New York, 124–125.

Fourar, M., Bories, S., Lenormand, R. and Persoff, P. (1993). Two-phase flow in smooth and rough fractures: measurement and correlation by porous-medium and pipe flow models. *Water Resources Res.*, **29**(11), 3699–3708.

Hu, Y.J. (2001). Experimental study on unsaturated seepage flow in fracture and numerical analysis of seepage flow in fractured rock mass due to surface infiltration (in Chinese). PhD Thesis Hohai University, Nanjing.

Hu, Y.J., Su, B.Y. and Zhan, M.L. (2001). Numerical analysis of saturated-unsaturated seepage flow in fractured rock mass due to surface infiltration. *J. Hydrodyn.*, **13**(4), 28–33.

Indraratna, B. and Ranjith, P.G. (2001). Laboratory measurement of two-phase flow parameters in rock joints based on high pressure triaxial testing. *J. Geotech. Geoenviron. Engng.*, **127**(6), 530–542.

Kwicklis, E.M. and Healy, R.W. (1993). Numerical investigation of steady liquid water flow in a variably saturated fracture network. *Water Resources Res.*, **29**(12), 4091–4102.

Liu, H.H. and Bodvasson, G.S. (2001). Constitutive relations for unsaturated flow in a fracture network. *J. Hydrol.*, **252**, 116–125.

Merrill, L.S. (1975). Two-phase flow in fractures. *PhD Thesis* University of Denver, Denver, CO.

Nicholl, M.J. and Glass, R.J. (1994). Wetting phase permeability in a partially saturated horizontal fracture. *Proceedings of the 5th International Conference on High Level Radioactive Waste Management*, American Nuclear Society, La Grange Park, USA Vol. 2, 2007–2019.

Persoff, P. and Pruess, K. (1995). Two-phase flow visualization and relative permeability measurement in natural rough-walled rock fractures. *Water Resources Res.*, **31**(5), 1175–1186.

Peters, R.R. and Klavetter, E.A. (1988). A continuum model for water movement in an unsaturated fractured rock mass. *Water Resources Res.*, **24**(3), 416–430.

Pieters, D.A. and Graves, R.M. (1994). Fracture relative permeability: linear or non-linear function of saturation. In: *Proceedings of the 1994 SPE International Petroleum Conference and Exhibition of Mexico*, Society of Petroleum Engineers, Richardson, USA, 333–342.

Pruess, K. (1998). On water seepage and fast preferential flow in heterogeneous, unsaturated rock fractures. *J. Contam. Hydrol.*, **30**, 333–362.

Reitsma, S. and Kueper, B.H. (1994R). Laboratory measurement of capillary pressure-saturation relationships in a rock fracture. *Water Resources Res.*, **30**(4), 865–878.

Romm, E.S. (1966). *Fluid Flow in Fractured Rocks* (in Russian). Nedra, Moscow.

Tokunaga, T.K. and Wan, J. (1997). Water film flow along fracture surfaces of porous rock. *Wat. Resources Res.*, **33**(6), 1287–1295.